



Int. J. New. Chem., 2025, Vol. 12, Issue 4, pp. 792-824.

International Journal of New Chemistry

Published online 2025 in <http://www.ijnc.ir/>.

Open Access

Print ISSN: 2645-7237

Online ISSN: 2383-188x



Original Research Article

Experimental Investigation and Modelling of Cold Plasma Effect on Microbial Load Reduction of Sumac (*Rhus coriaria* L) by Artificial Neural Network with Levenberg–Marquardt Algorithm

Somayeh Sepahvand¹, Nastaran Khalaj Zeighami² and Samaneh Tayebi-Moghaddam²

¹Department of Food Science and Technology, Islamic Azad University, Yasouj Branch, Yasouj, Iran

²Department of Food Science and Technology, Islamic Azad University, Science and Research Branch, Tehran, Iran.

Received: 2024-11-13

Accepted: 2025-02-22

Published: 2025-02-23

ABSTRACT

In this study, the application of dielectric barrier discharge (DBD) cold plasma with gases (air and nitrogen) for a duration of 15 minutes on the surface of sumac samples was investigated experimentally to reduce the microbial load. The sumac samples were subjected to two treatments: plasma treatment for 15 minutes and exposure to different gases (Nitrogen and Oxygen) at two levels. Immediately after the treatments, their microbial load was measured. Furthermore, the experimental results will be modeled using artificial neural networks. The results of the microbial tests showed that the antimicrobial effect of nitrogen plasma was lower compared to air plasma, and the duration of plasma irradiation had a significant effect on microbial load reduction. With an increase in the duration of plasma irradiation, the inactivation of microorganisms increased, and the maximum reduction in microbial load was observed at 15 minutes of exposure to air plasma.

Keywords: Cold plasma, Microbial load, Sumac, Levenberg–Marquardt Algorithm

Introduction

Foodstuffs can undergo various changes and spoilage during storage. This spoilage can affect the food's taste, color, texture, hygiene, and nutritional value. It should be noted that food ingredients and components are sensitive and prone to detrimental reactions that can occur quickly under environmental factors such as oxygen, light, microorganisms, and moisture, leading to unintended changes in food items [1]. Spices are plant-based products used to enhance the flavor and taste of foods[2]. These products can become contaminated with various microorganisms during harvesting, drying, and transportation processes. Currently, various physical methods such as freezing [3], drying [4], heat treatment [5], packaging [6], and chemical processes such as the addition of various additives are widely used for food preservation[7]. The essential methods of food preservation include heat treatment, refrigeration, reduction of relative humidity, fermentation, use of preservatives, and irradiation [8]. Cold plasma can sterilize inactive microorganisms, including spores, bacteria, molds, and yeasts. In addition, the current method is a suitable option for disinfecting heat-sensitive products such as spices and medicinal plants due to its advantages of no waste generation, lower energy consumption and cost, as well as preservation and improvement of nutritional properties [9]. Plasma can have preference over other methods for surface decontamination of spices without causing qualitative damage. Although widely used in the food industry, thermal processing can adversely affect the quality, physicochemical properties, and sensory attributes of heat-sensitive spices. The application of high temperatures may lead to tissue damage and nutrient loss, compromising the overall nutritional value of the spices[10]. In order to minimize such undesirable effects, non-thermal technologies have emerged as alternative or complementary approaches to traditional thermal treatments in the food industry. These technologies aim to effectively sterilize of spices while preserving their sensory and nutritional characteristics by utilizing chemical and physical methods that do not rely on excessive heat. This shift towards non-thermal techniques reflects a growing demand for food processing methods that maintain heat-sensitive ingredients' quality and nutritional value, such as spices[11]. Non-thermal technologies such as pulsed electric fields, radio frequency, high hydrostatic pressure, ultrasound, supercritical carbon dioxide, electrolyzed oxidizing water, oscillating magnetic fields, and cold plasma (CP) have been recognized as effective methods in food processing. Unlike conventional thermal operations, these processes are conducted at ambient temperature,

thereby minimizing the undesirable effects on food products [12]. Plasma treatment assists in microbial inactivation through its interaction with biological materials. Plasma treatment has a broad spectrum of activity against microorganisms, including bacteria and viruses. Reactive species present in plasma, including O₂, OH, NO, NO₂, and others, are known to exert direct oxidative effects on the outer surface of microbial cells. It is hypothesized that active oxygen species significantly impact membrane lipids, as they are close to the bacterial cell surface and can effectively interact with these potent oxidizing Agents Sumac is a valuable natural resource known for its diverse range of compounds that have applications in various industries including pharmaceuticals, food, and textiles. Using sumac as a natural preservative in the food industry is effective due to its antioxidant, antifungal, and antibacterial properties[13]. More specifically, greater attention should be given to the potential use of sumac powder as a preservative in red meat and poultry. In addition, using sumac extract as a natural supplement or seasoning provides a desirable sour taste, which is an alternative to the synthetic compounds like citric acid that are commonly used for this purpose. Another critical aspect of sumac is its potential to provide important phytochemicals beneficial for health, with antioxidant and anti-obesity potential for consumers[14–17]. Additionally, the rich tannin content, high availability, and low cost of sumac powder make it an interesting option as an inexpensive dye in the textile industry[18,19]. Furthermore, due to its numerous medicinal properties such as anticancer, anti-inflammatory, neuroprotective, analgesic, cardioprotective, and antidiabetic effects, the scientific and pharmaceutical community has shown greater interest in utilizing this plant as a source for new bioactive compounds[20,21]. To evaluate and analyze the effects of plasma gas, both experimental and theoretical modeling methods have been employed[22]. Practical methods utilize precise laboratory instruments and equipment, providing reliable and trustworthy results when used correctly. However, experimental methods require specialized facilities and equipment, leading to high financial and time costs. Therefore, modeling methods and algorithms can be alternatives to practical approaches [23,24]. Modeling in engineering and related sciences involves the use of mathematics, physics, and computer simulations to analyze and predict critical parameters[25,26]. Through modeling, the effects of various parameters on the performance of a method can be examined relative to the laws of physics and mathematics. Some of these methods include numerical modeling and artificial intelligence modeling[27]. Artificial neural networks have been recognized as a powerful tool In The field of modeling and

prediction of various systems in the food industry[28–30]. Using this method, researchers can design and predict multiple properties of substances and different preservation systems[31–33]. Using artificial neural networks in modeling preservation systems offers advantages such as high-speed processing, more accurate predictions, and applicability to complex problems[34]. With its high predictive power and accuracy, this approach allows researchers to investigate and implement necessary improvements and optimizations in preservation systems. Furthermore, artificial neural networks have the ability to interact with laboratory and experimental data, enabling the development of more accurate models and the examination of required features for preservation systems[35]. In this study, the effect of dielectric barrier discharge (DBD) plasma using gases (air and nitrogen) was investigated on the surface of sumac samples for a plasma treatment duration of 15 minutes, aiming to reduce microbial load (*Escherichia coli*, *Bacillus cereus*, and mold) through experimental analysis. In continuation of the studies conducted on the role and functionality of artificial neural networks, in this study, the prediction of the microbial load under different gas treatment conditions and at different time intervals on the sample will be carried out using a multilayer perceptron. The artificial neural network will be utilized model and predict microbial load under various gas application conditions on the model. In the initial phase, an experimental investigation of the effect of nitrogen gas and air on the reduction of microbial load in the sample will be conducted. The following section will focus on the design of the artificial neural network, including the introduction of the functions used in the model and the specifications of the layers and neurons in each layer. Finally, an analysis of the gas effect on the desired properties, as well as the accuracy and performance of the model using statistical indices, will be discussed.

1. Experimental Investigation

1.1. Materials and preparation method

Clusters of sumac fruits (*Rhus coriaria* L), along with their branches and leaves, were collected from sumac cultivation fields in the Boein-Zahra region of Qazvin province, Iran. The necessary part for conducting the research, the sumac fruit, was separated from the clusters and other excess parts. It was then dried and used for the intended experiments. The drying process was carried out using traditional methods, relying on sunlight. After drying, the sumac fruits were manually ground using a grinder, where the skin and fruit were ground together. Once the sumac powder was prepared, its microbial load was determined. The microbial test results indicated that the sumac sample falls within the standard range of microbial load. To further assess its microbial contamination, samples were tested for *Escherichia coli*, *Bacillus cereus*, and *Aspergillus niger* to assess microbial contamination further. Each sample was divided into two groups for chemical and microbial experiments. To preserve the quality of the sumac powder until the chemical and microbial tests were conducted, the samples were stored in dark-colored glass containers, protected from moisture, at a temperature of 4 degrees Celsius.

The indicator microorganisms used in this research were *Escherichia coli* and *Bacillus cereus*. The lyophilized bacteria were inoculated linearly into a specialized nutrient broth culture medium and incubated at 37 degrees Celsius for 24 hours. Then, in two consecutive stages, they were separately inoculated into a nutrient agar culture medium and incubated at 37 degrees Celsius for 24 hours. The nutrient agar culture medium was centrifuged at 4,000 RPM for 15 minutes at 22 degrees Celsius to separate the bacteria from the culture medium. The resulting bacterial sediment was washed with peptone water (0.1 grams of peptone in 100 milliliters) in three stages and centrifuged at 4,000 RPM for 15 minutes. The sumac samples without bacteria were placed in sterile petri dishes for inoculation, and 150 microliters of each indicator microorganism were aseptically inoculated onto the sumac under laminar hood conditions. The inoculated powder was dried at 22 ± 2 degrees Celsius for one hour. The prepared mold was inoculated onto plates containing yeast extract-glucose-chloramphenicol agar medium (YGC)

and incubated in an incubator at 25-27 degrees Celsius for 3 to 5 days to allow for the formation of black-colored hyphae. Then, using forceps, a portion of the black hyphae was taken and placed in a sterile distilled water solution. Subsequently, the hyphae were counted using a light microscope under a Neubauer chamber. Finally, the mold was inoculated onto the Sumac samples under sterile conditions and a laminar hood.

1.2. Test Procedure

For microbiological testing of sumac, sampling was carried out according to ISO 948:1980 [36]. The sumac samples were subjected to two treatments: plasma treatment for 15 minutes and exposure to different gases (Nitrogen and Oxygen) at two levels. Immediately after the treatments, their microbial load was measured. According to ISO 6887-1:2017 [37], 10 grams of sumac were weighed under a sterile hood using a digital balance to prepare the samples for microbiological testing. They were then combined with 90 milliliters of sterile diluent (Ringer's) solution to obtain an initial suspension. The samples were homogenized by shaking in a 1 cc shaker using a 1 cc sampler under sterile conditions. The homogenized mixture was transferred to sterile test tubes containing 9 cc of sterile Ringer's solution. This process was repeated for a total of nine stages of dilution.

The surface culture method adds approximately 15-20 milliliters of the respective culture media to the plates. After sealing the culture media, 100 microliters of the samples are poured onto the plates using a pipette. The samples are evenly spread on the culture media using a bent glass rod. Then, the inoculated plates are placed at 25 degrees Celsius for 3 days. In the mixed or pour plate method, 1000 microliters of the samples are poured onto the plate surface, followed by adding approximately 15-20 milliliters of the respective culture media at 49-50 degrees Celsius. The mixture is thoroughly mixed by making figure-eight rotations. The inoculated plates using this method are incubated at 37 degrees Celsius for 2 days. Each treatment is replicated twice. After incubation, the colonies are counted within 15-300 colonies per plate. Finally, the microbial load is calculated in terms of Log cfu/g using the following equation. The counting of microorganisms in this study was performed using various international standards. The following is an explanation of the method used: Escherichia coli count: According to ISO 7251:2005 [38], the test was conducted using the Eosin Methylene Blue (EMB) culture medium. The plates were

prepared, and after closing the culture medium, they were inverted and incubated at 37 °C for 24 hours in an incubator. At the end of the incubation period, each plate containing colonies with a green metallic sheen was identified and counted. *Bacillus cereus* count: According to ISO 7932:2004 [39] , the test was conducted using the sterile MYP (Manitol-egg yolk-polymyxin agar) culture medium. 1 ml of the initial suspension was poured onto the surface of two 14 cm agar plates containing MYP culture medium, or 0.3 ml onto the surface of six 9 cm agar plates. For decimal dilutions, using another pipette, 1 ml of the 10⁻² dilution was poured onto the surface of a 14 cm agar plate (0.3 ml onto 9 cm plates). The above method was repeated for subsequent decimal dilutions using a separate pipette for each dilution. The inoculum was evenly spread on the culture medium's surface without contacting the plates' edge. The plates were kept at room temperature for 15 minutes, allowing the inoculum to be absorbed into the culture medium's surface. Then, the prepared plates were inverted and incubated at 30°C for 18 to 24 hours. After incubation, plates with less than 150 colonies from consecutive dilutions were selected. Large, pink colonies (indicating mannitol non-fermenting) with precipitate halos (indicating lecithinase production) were counted as potential *Bacillus cereus*. Still, some strains of *Bacillus cereus* produced no or low lecithinase, resulting in colonies without precipitates. A confirmatory test was performed for these colonies. The selected colonies were linearly streaked on the surface of blood agar plates and then incubated at 30°C for 2 ± 24 hours. In the hemolysis test, if clear halos were present around the colonies on the blood agar medium, the test was considered positive, and the probable count of *Bacillus cereus* was calculated using a specific formula. Mold count: According to ISO 21527-2:2008[40] , the test was conducted using the sterile Dichloran 18% mass fraction glycerol agar (DG18) culture medium. A specified amount of the initial suspension was poured onto the surface of DG18 plates (to prevent bacterial growth, the presence of chloramphenicol and glycerol in the culture medium is necessary) using the surface plating method. The plates were then incubated aerobically at (25±1)°C for 5-7 days. The number of molds and yeasts in colony-forming units (CFU) per gram or milliliter of the sample was calculated based on the counts of colonies, propagules, or visible growth on the selected plates from dilutions that yielded the best results.

2. Artificial Neural Network Modelling

Until today, ideas and inspirations derived from nature and living systems have always been considered fundamental principles in solving various problems and have led to significant achievements. Initial efforts to model the brain and human neural networks have resulted in the development of models for the functioning of a brain processing unit, known as a neuron. Artificial neural networks (ANNs), which are represented by the term ANN, are composed of units called neurons[41]. Neurons in a neural network act as the main processors. Figure 1 demonstrates how an artificial network operates based on input and output parameters, and the role and position of the functions used in modeling[42].

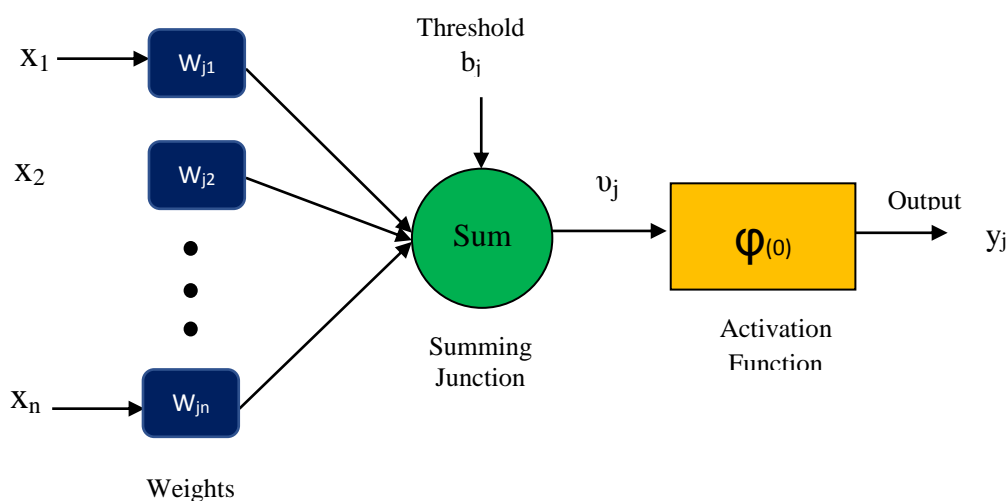


Figure 1. Schematic diagram of a neuron

In this diagram, x_i represents the input parameters of the network, and n represents the number of input parameters. Additionally, j represents the number of neurons in the neural network, and w_{ji} represents the synaptic weight from neuron i to neuron j , indicating the strength of the connection between them. The linear combination output, u_j , is also considered, which is equal to[43]:

$$u_j = \sum_{i=1}^n w_{ji} x_i \quad (1)$$

$$y_j = \varphi(u_j + b_j) \quad (2)$$

$$v_j = u_j + b_j \quad (3)$$

Where $\varphi(0)$ is the activation function and b_j is the bias term of the function. Various activation functions have been used in previous studies. In this study, the Log-sigmoid and Tangent sigmoid activation functions were used for the hidden layers, while the Purelin function was used for the output layer. These functions are specified as follows[44]:

$$\text{tansig}(x) = \frac{2}{1 + \exp(-2x)} - 1 \quad (4)$$

$$\text{logsig}(x) = \frac{1}{1 + \exp(-x)} \quad (5)$$

$$\text{purelin}(x) = x \quad (6)$$

Where x is considered as the input to the activation function.

In general, an artificial neural network acts as a function, receiving input variables based on the number of neurons in the input layer and producing output based on the number of neurons in the output layer. In this study, the input parameters include time and the type of input gas, which are placed in the first layer. Considering the weights associated with the neurons and the different numbers of neurons in the hidden layers, the microbial load is regarded as the network's output in the final layer.

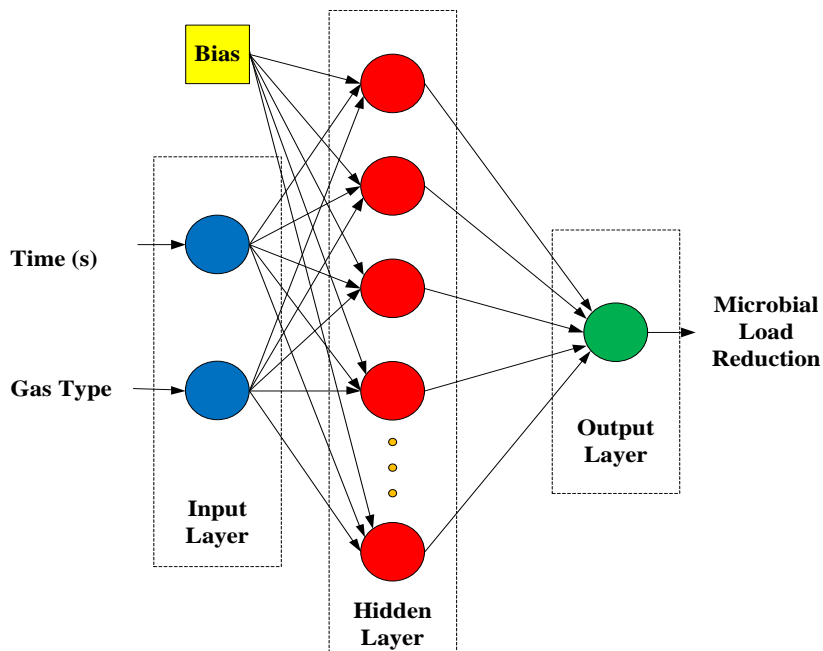


Figure 2. Schematic of the ANN structure for predicting the microbial load reduction

This study's modeling was performed using a neural network with MATLAB a2023 software. The input parameters of the network, which were experimentally measured and used for training the network, consisted of 1445 samples. These samples were normalized within the range of -1 to 1 using the following equation and then utilized on the web[45]:

$$y = 2 \times \left(\frac{x - x_{min}}{x_{max} - x_{min}} \right) + 1 \quad (7)$$

3. Statistical analysis

This study used statistical indicators to measure the accuracy and performance of the model and the neural network. The root mean square error (RMSE), mean absolute percentage error (MAPE), coefficient of determination (R^2), and mean bias error (MBE) were employed as

appropriate indicators to determine the accuracy of the model. The RMSE, MAPE, and MBE are suitable indicators for assessing the accuracy of the model, where a lower value indicates a higher accuracy. The coefficient of determination (R^2) represents the likelihood of correlation between two data sets in the future. A value close to one indicates a better performance of the model. The equations used to calculate these indicators are defined as follows[46]:

$$RMSE = \sqrt{\frac{1}{n} \sum_{i=1}^n (\eta_p - \eta_a)^2} \quad (8)$$

$$MAPE = \frac{1}{n} \sum_{i=1}^n \left| \frac{(\eta_p - \eta_a)}{\eta_a} \right| \times 100 \quad (9)$$

$$R^2 = 1 - \frac{\sum_{i=1}^n (\eta_a - \eta_p)^2}{\sum_{i=1}^n (\eta_a - \bar{\eta}_a)^2} \quad (10)$$

$$MBE = \frac{1}{n} \sum_{i=1}^n (\eta_p - \eta_a) \quad (11)$$

Where η_p is the predicted outlet and η_a is the actual measured. The average measured outlet, $\bar{\eta}_a$ is evaluated using the measured period and sample number.

Results and Discussion

Experimental Results

Based on Figure 3, the population of E. coli inoculated with air gas for 15 minutes showed a significant difference ($P < 0.05$) compared to other samples. In general, with increasing time, a further reduction in microbial load was observed in the samples. E. coli is a gram-negative bacterium surrounded by a thin peptidoglycan layer and an outer lipopolysaccharide membrane. Reactive oxygen and nitrogen species generated in the plasma can interact with the lipopolysaccharide and peptidoglycan of E. coli, disrupting CON, COO, and COC bonds and destroying E. coli's structure.

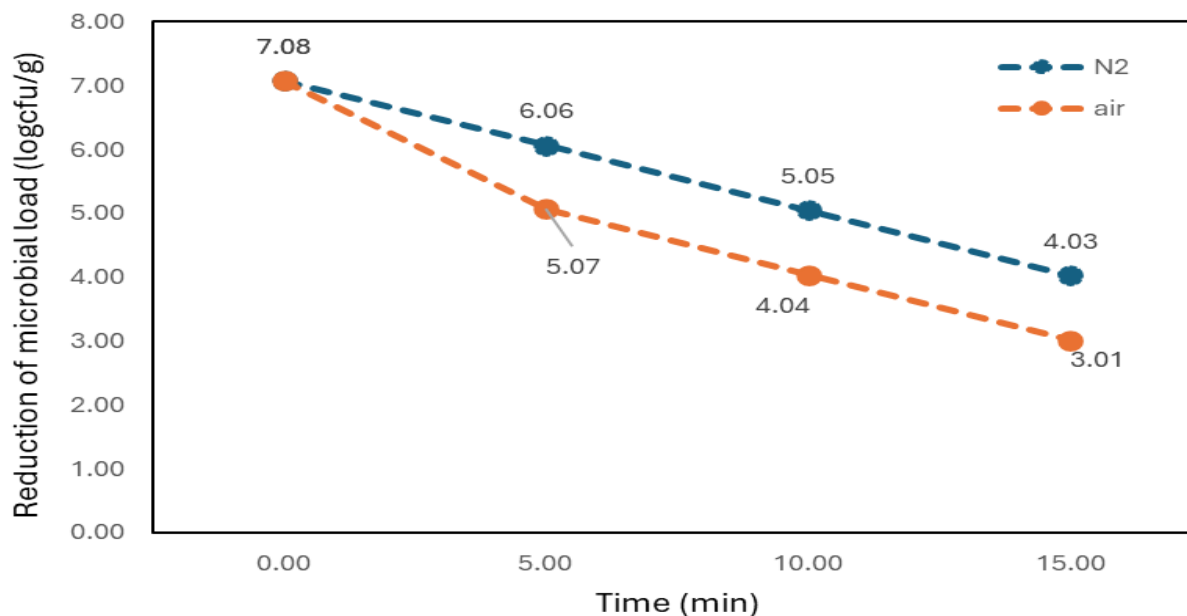


Figure 3. The variable effect of time and gas on reducing *Escherichia coli* microbial load

The effect of air plasma (consisting of 78% nitrogen and 20% oxygen) on *Escherichia coli*'s inactivation was significantly greater than nitrogen plasma. The gas used for plasma generation plays an important role in the inactivation of microorganisms. The type of gas composition can influence the types and ratios of reactive species produced. Oxygen reactive species and nitrogen reactive species alone may have a lesser effect on microbial reduction. Figure 4 illustrates the changes in the reduction of *Bacillus cereus* at 0, 5, 10, and 15 minutes. As the plasma irradiation time increased, the level of *Bacillus cereus* inoculated on sumac significantly decreased, and the most significant reduction occurred between 5 to 10 minutes. Cold plasma generates antimicrobial species such as ultraviolet radiation and active species (radicals, excited atoms, and molecules). Microorganisms are eliminated by contacting these antimicrobial active species during the irradiation process.

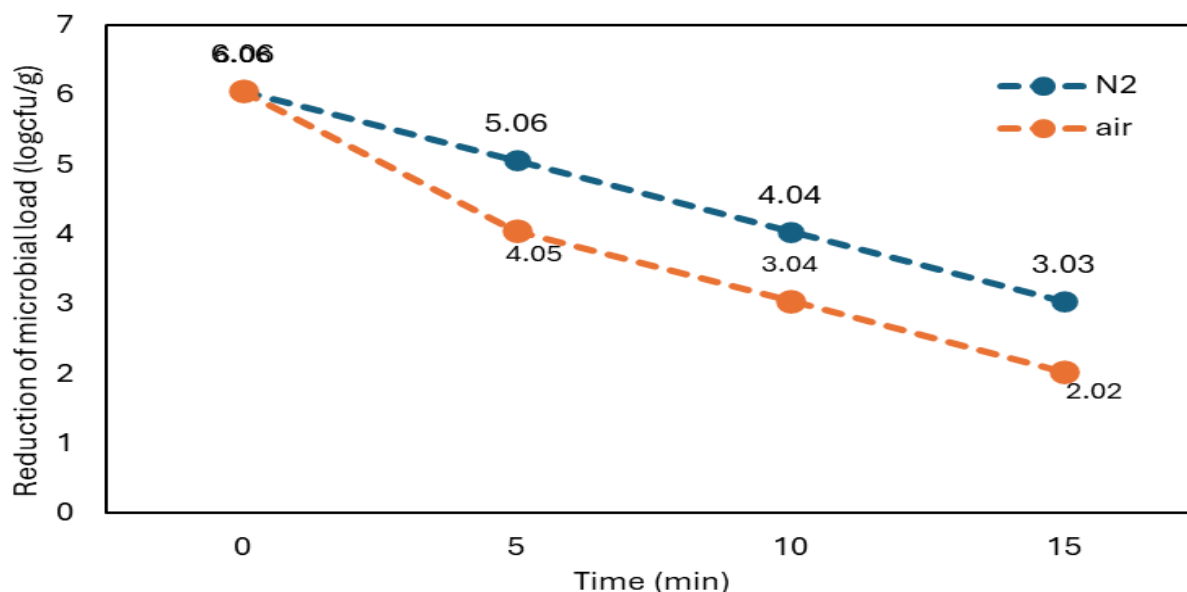


Figure 4. The variable effect of time and gas on reducing *Bacillus cereus* microbial load

As mentioned, cold plasma induces the production of reactive oxygen species, reactive nitrogen species, and ultraviolet radiation. These species initially act on the cell wall and membranes of microorganisms. After damaging the cell wall, the reactive species penetrate the cell, leading to oxidation, cellular damage, and ultimately cell death. Therefore, the difference in the thickness of the peptidoglycan layer between Gram-positive bacteria (20-30 nanometers) and Gram-negative bacteria (6 to 7 nanometers) results in different rates of inactivation and varying effects of plasma on the cell wall. As observed in Figure 4, air plasma (composed of 78% nitrogen and 20% oxygen) had a greater impact on *Bacillus cereus*'s inactivation compared to nitrogen plasma alone. This difference was statistically significant. Plasma generated with nitrogen gas (N₂) contains reactive nitrogen species (RNS). Reactive nitrogen species can oxidize lipids, proteins, and DNA of microorganisms, causing damage to the cellular structure. As shown in Figure 5, the effect of plasma irradiation time on the fungal population is depicted. The fungal population significantly decreased with increasing irradiation time. No significant difference was observed among the treated samples at different time points, but there was a significant difference between the control samples and the treated samples. The highest level of fungal inactivation was observed at 5 to 10 minutes of irradiation time.

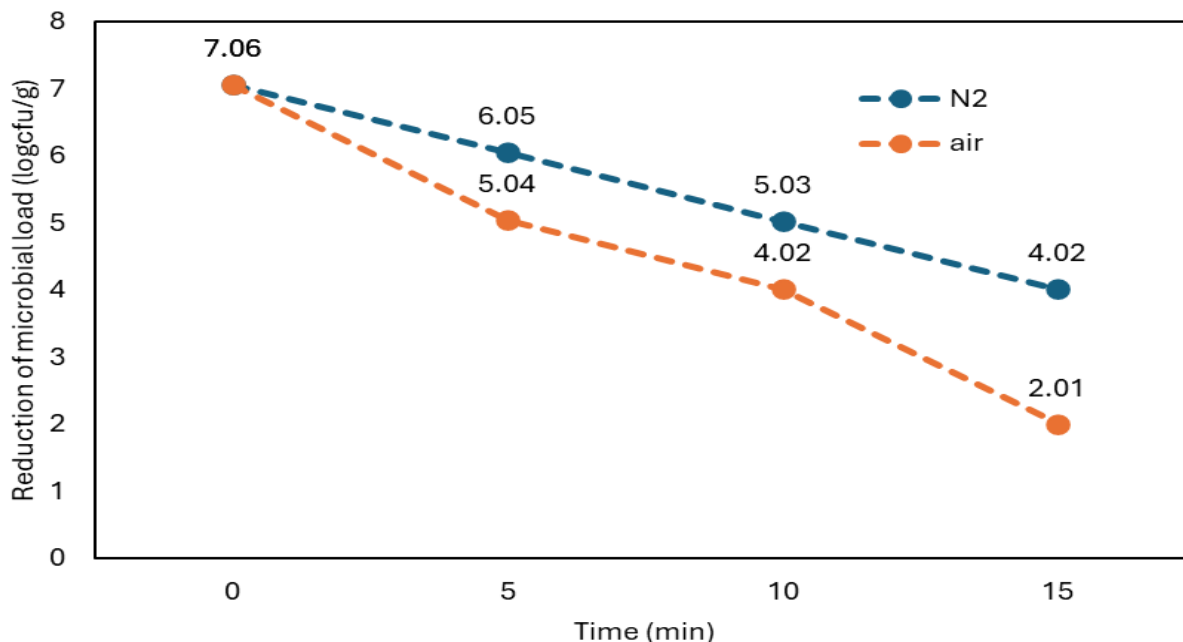


Figure 5. The variable effect of time and gas on reducing mold microbial load

As observed, the average reduction in *Escherichia coli* and *Bacillus cereus* populations was higher compared to fungi. This difference could be due to fungi's thicker cell wall structure than bacteria's peptidoglycan membrane. In this study, *Escherichia coli* showed greater sensitivity to cold plasma radiation with both types of gas compared to *Bacillus cereus*. In such cases, it can be attributed to a stronger protein reaction than lipids. Based on this hypothesis, the higher amount of protein in the cell wall of Gram-negative bacteria may lead to their greater sensitivity to plasma radiation compared to Gram-positive bacteria. Additionally, the cell wall of Gram-positive bacteria contains a thick layer of peptidoglycan, while Gram-negative bacteria are covered with a thin layer of peptidoglycan. This difference in cell wall structure can contribute to the higher inactivation of *Escherichia coli*. The results in Figure 6 demonstrate that the effect of gas type and duration of plasma treatment on microbial load reduction was statistically significant at a 5% confidence level ($P < 0.05$). However, for the reduction of fungal load, only the duration of treatment had a significant effect, and the reduction rate in samples treated with nitrogen plasma was slightly lower than those treated with air plasma (78% nitrogen + 20% oxygen). The results indicate that plasma treatment with air gas for 15 minutes is the most effective condition.

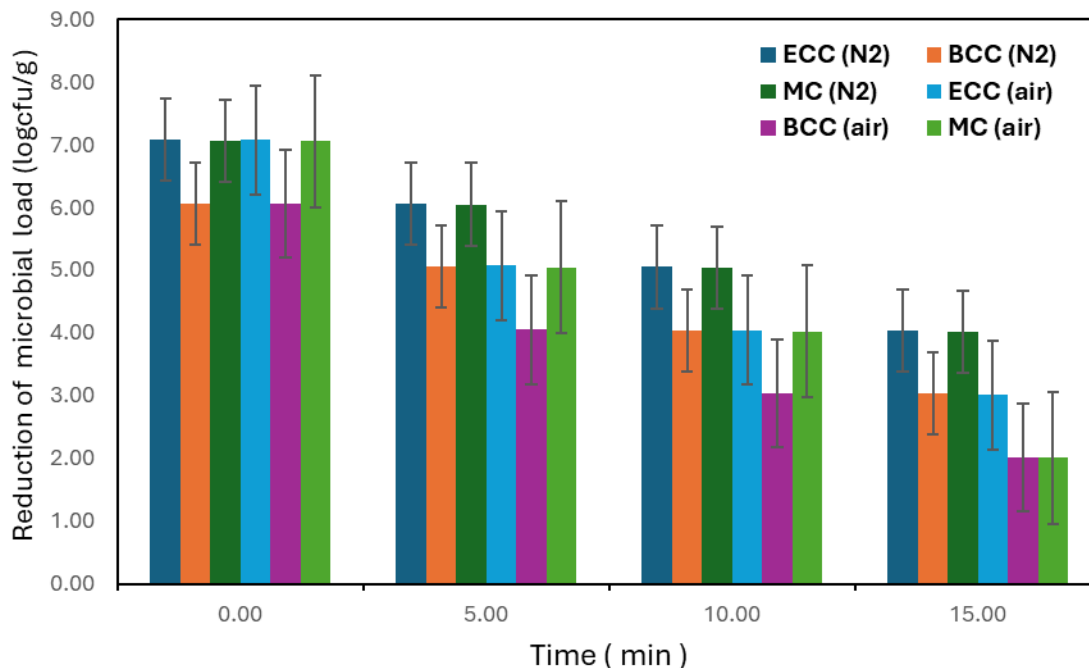


Figure 6. The graph of reducing the microbial load of sumac samples under the effect of gases and different times

Modelling Results

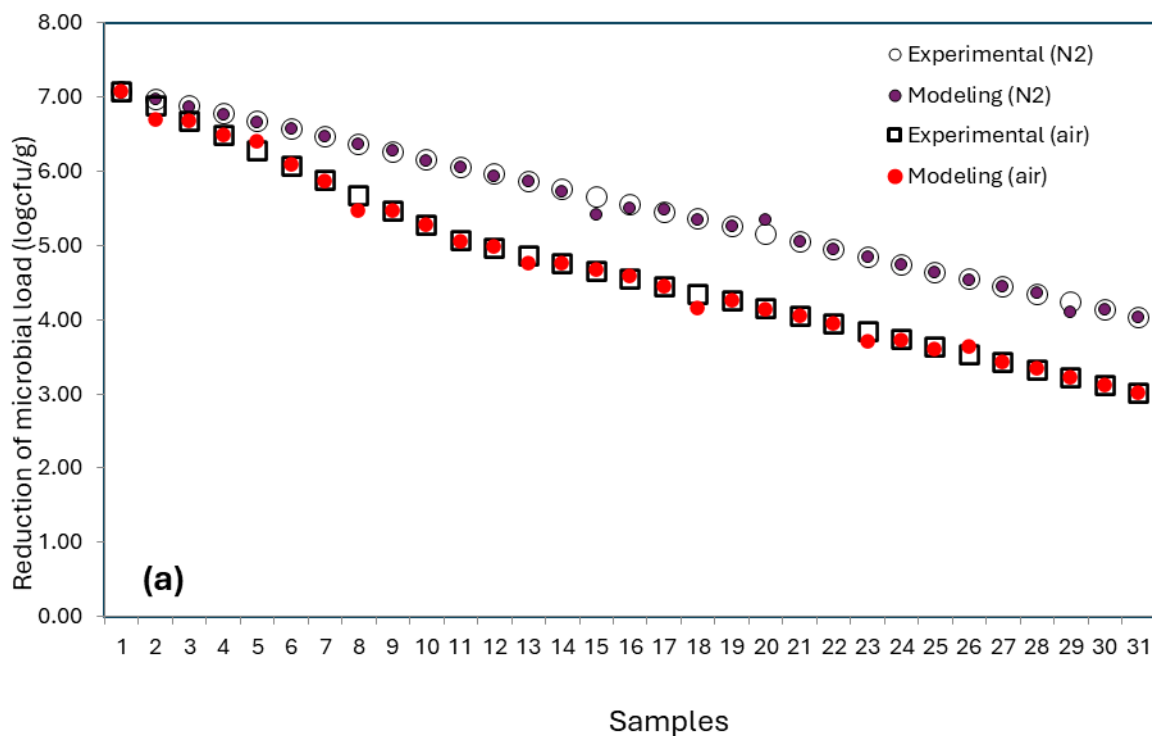
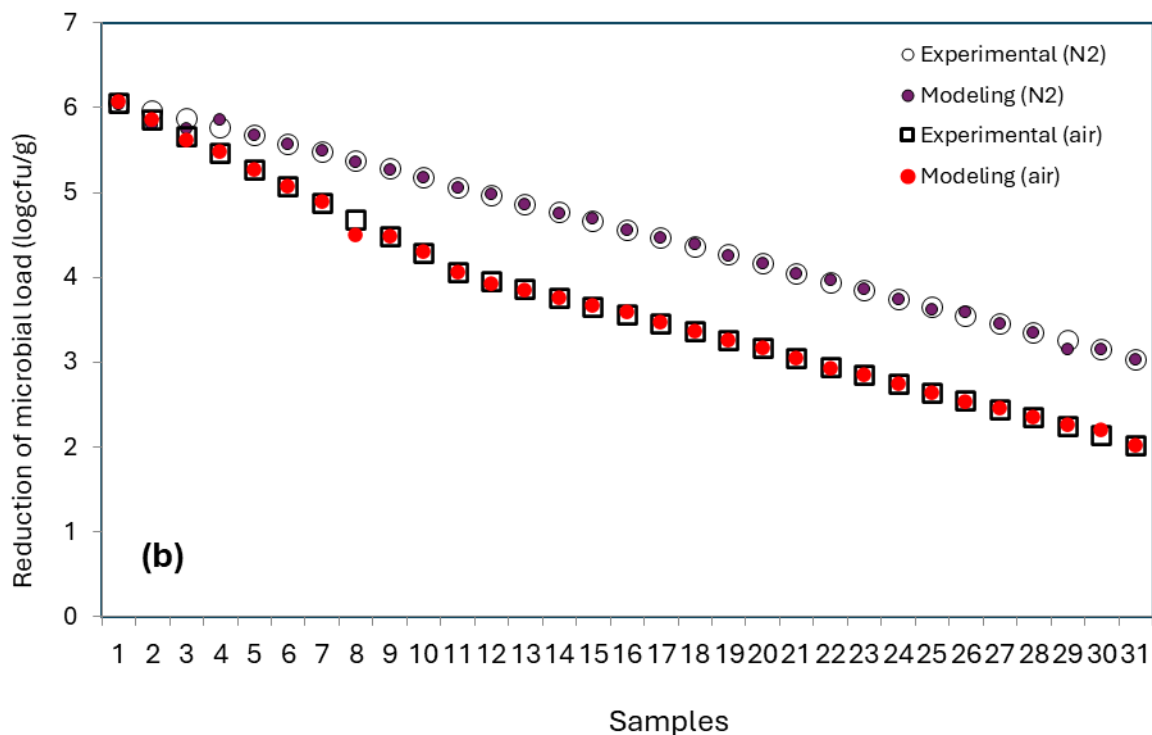
According to the prediction method mentioned in Section 4, the modeling was performed using an artificial neural network. In this stage, a trial and error approach was employed, where the number of neurons, layers, and network functions were modified in each modeling iteration. The results regarding the accuracy and performance of the model, and the statistical indicators, were recorded. The obtained results are presented in Table 1.

Table 1. The results of model accuracy measurement indices under different condition

Models	Functions	Neurons	MAPE	RMSE	R ²	MBE
ANN-1	Tan-sigmoid, Tan-sigmoid, Purelin	2,10,1	0.405	0.031	0.998	-0.013
ANN-2	Tan-sigmoid, Tan-sigmoid, Purelin	8,12,1	0.13	0.029	0.997	0.0015
ANN-3	Tan-sigmoid, Tan-sigmoid, Purelin	12,22,1	0.008	0.029	0.998	0.0002
ANN-4	Tan-sigmoid, Log-sigmoid, Purelin	5,9,1	1.62	0.082	0.991	-0.0005
ANN-5	Tan-sigmoid, Log-sigmoid, Purelin	8,16,1	0.21	0.05	0.997	0.0012
ANN-6	Log-sigmoid, Log-sigmoid, Purelin	7,14,1	1.44	0.055	0.992	-0.005
ANN-7	Log-sigmoid, Log-sigmoid, Purelin	8,24,1	0.29	0.025	0.996	-0.006
ANN-8	Log-sigmoid, Tan-sigmoid, Purelin	10,16,1	0.58	0.02	0.996	0.007
ANN-9	Log-sigmoid, Tan-sigmoid, Purelin	4,4,1	1.12	0.51	0.994	0.009
ANN-10	Tan-sigmoid, Purelin	10,1	1.65	0.058	0.991	0.005
ANN-11	Tan-sigmoid, Purelin	4,1	2.53	0.09	0.988	-0.008
ANN-12	Log-sigmoid, Purelin	2,1	2.44	0.09	0.989	0.001
ANN-13	Log-sigmoid, Purelin	12,1	1.49	0.073	0.995	-0.0015

Based on the results presented in Table 1, the most optimal model with higher accuracy and reliability is selected. Among the mentioned activation functions, the optimal model utilizes the tansig function in the first and second hidden layers and the purelin function in the output layer. It is important to consider computational efficiency to determine the optimal number of neurons and layers. Increasing the number of neurons and layers can significantly increase the computational time required for modeling. In this regard, the optimal number of neurons in the first layer is determined to be 12, and in the second layer, it is 22, based on the ANN-3 model. Since the objective is to predict a single parameter, the final layer will have one neuron dedicated to this output parameter. This design ensures that the model focuses on accurately predicting the desired output variable. By selecting the most optimal model configuration, including the appropriate activation functions, number of neurons, and layer architecture, the model achieves

enhanced accuracy and reliability in predicting microbial load reduction. The output results obtained from the trained Artificial Neural Network (ANN) model exhibit a strong agreement with the experimental data, as demonstrated by the substantial overlap of the data points in Figure 7. This indicates that the ANN model effectively captures the underlying patterns and trends in the data. Several statistical indices were considered to assess the model's accuracy and reliability. Among these, the absolute mean error index plays a crucial role. A value below 10% suggests a high level of accuracy, indicating that the model's predictions closely align with the actual experimental values. Additionally, other statistical measures, except for R^2 (coefficient of determination), are also expected to be close to zero for a reliable model. These measures include root mean square error (RMSE), mean absolute error (MAE), and mean deviation error. When these measures approach zero, it indicates that the model's predictions exhibit minimal deviation from the experimental data, further emphasizing the model's accuracy and reliability. Overall, the close agreement between the output results of the ANN model and the experimental data, coupled with the favorable statistical indices, reinforces the model's effectiveness and its ability to accurately represent the studied phenomena. The ANN-3 model has an absolute mean error of 0.008% (much less than 10%), an RMSE of 0.029, a correlation coefficient of 99.8%, and a mean error of only +0.0002.



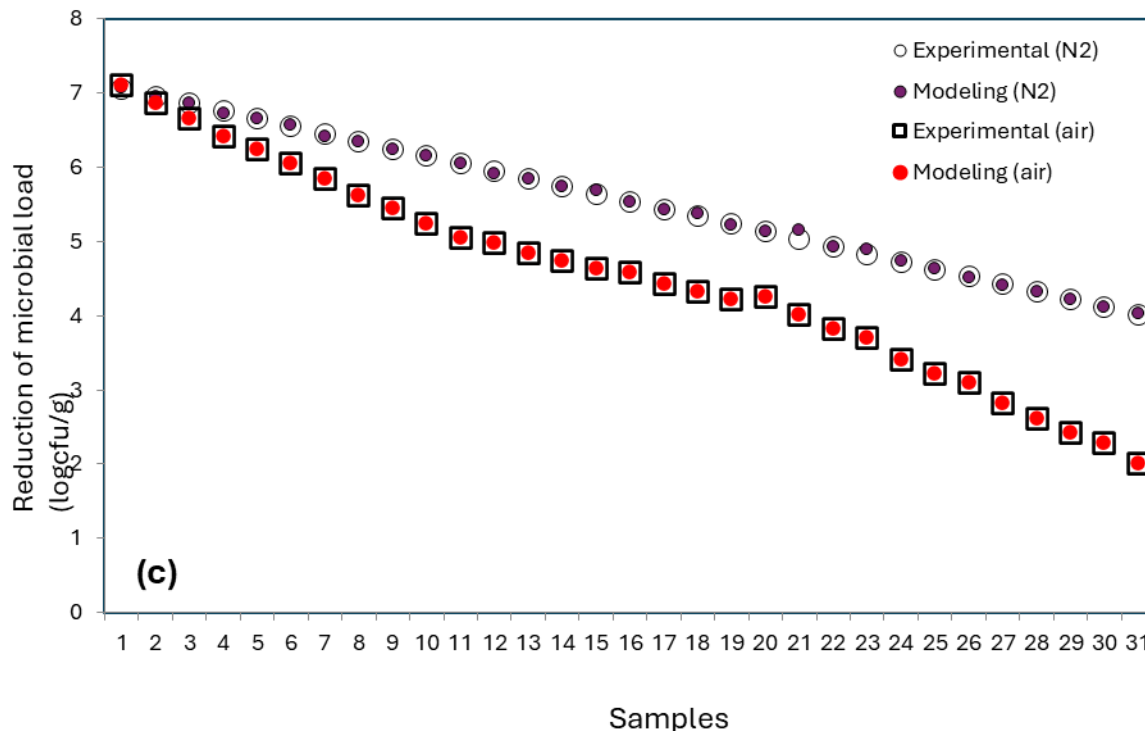


Figure 7. Comparison of Experimental Results and Predicted Values by Artificial Neural Network

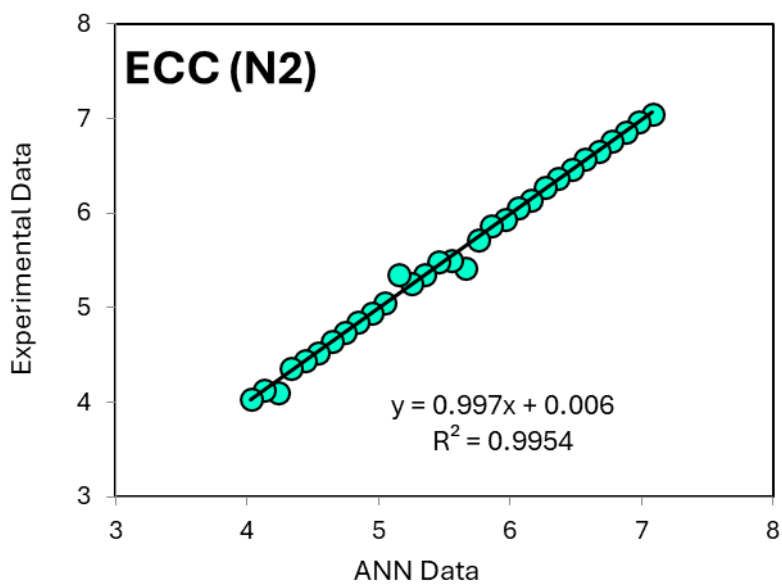
a) Escherichia Coli Count (ECC) b) Bacillus Cereus Count (BCC) c) Mold Count (MC)

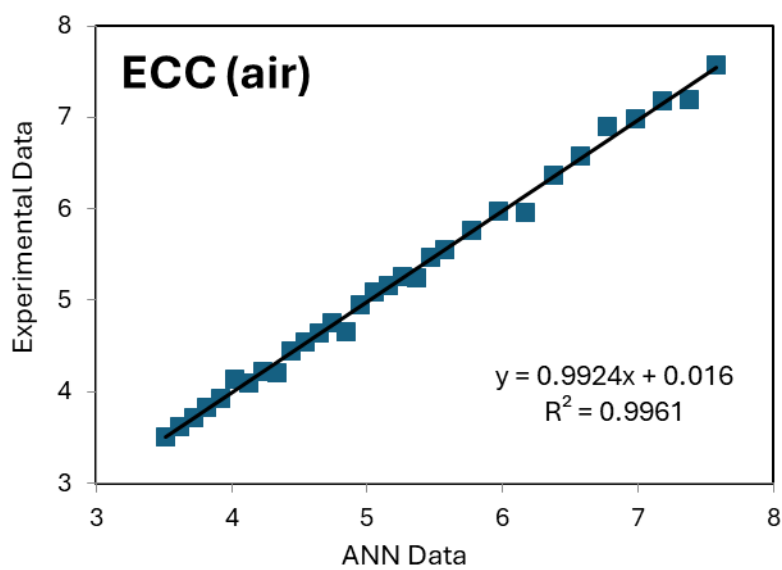
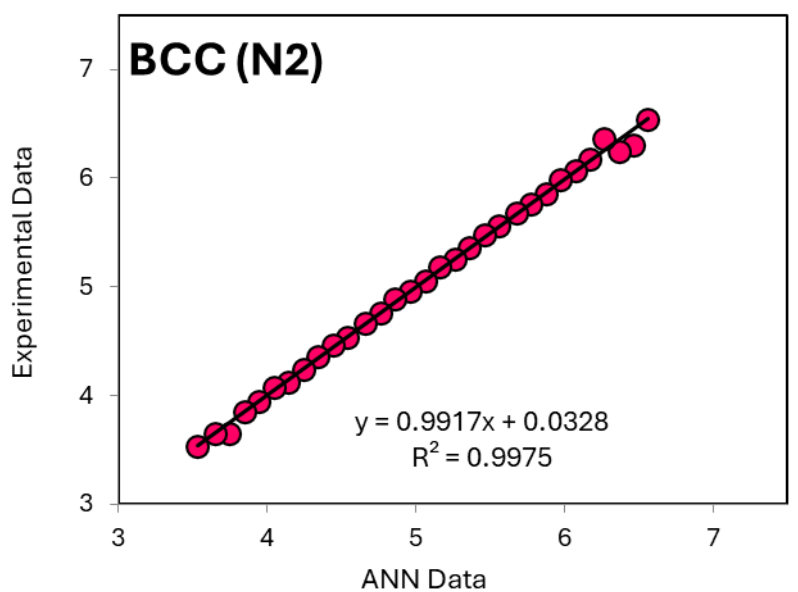
Correlation analysis is a statistical tool used to determine the nature and strength of the relationship between two quantitative variables. The correlation coefficient is commonly used to assess the correlation between two variables. It indicates the strength and direction (positive or negative) of the relationship. The correlation coefficient ranges from -1 to 1.

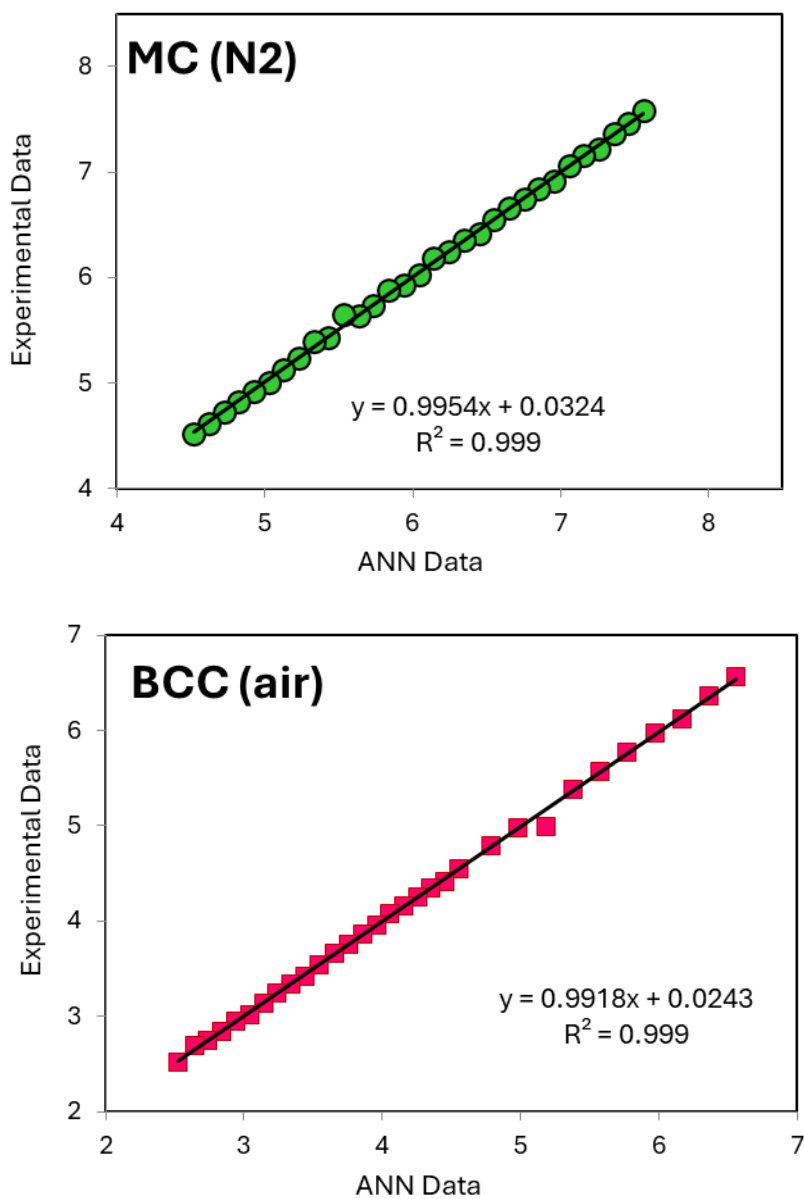
A value of 1 indicates a perfect positive correlation, meaning that as one variable increases, the other variable also increases proportionally. A value of -1 indicates a perfect negative correlation, indicating that as one variable increases, the other variable decreases proportionally. A correlation coefficient of 0 suggests no linear relationship between the variables. It is important to note that correlation analysis assesses the linear relationship between variables and may not capture non-linear relationships

The correlation coefficient only measures linear relationships. Therefore, a correlation coefficient of zero indicates that there is no linear relationship between variables x and y , but it is possible that they have a non-linear relationship. By squaring the correlation coefficient, we

obtain the coefficient of determination (R^2), which represents the percentage of variance in the dependent variable explained by the independent variable. The correlation plot between the experimental measurements and the model predictions is shown in Figure 8.







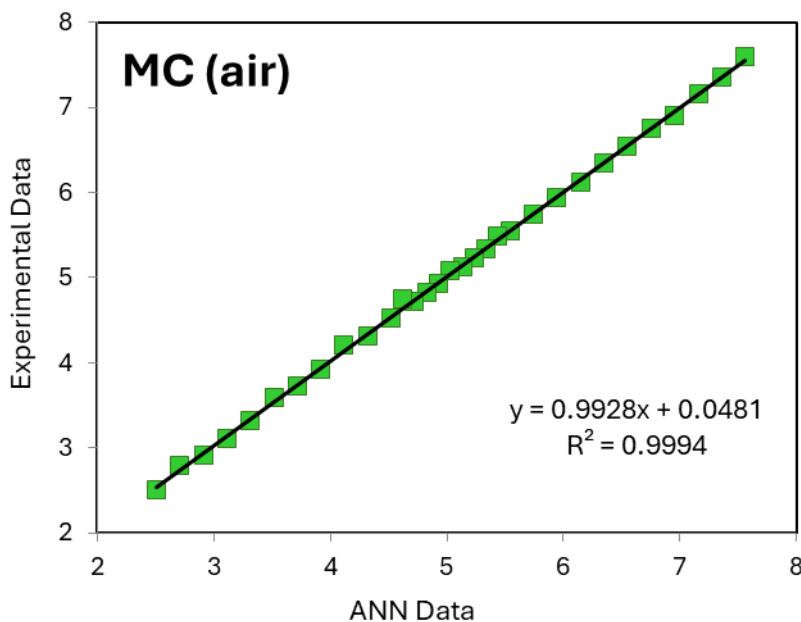
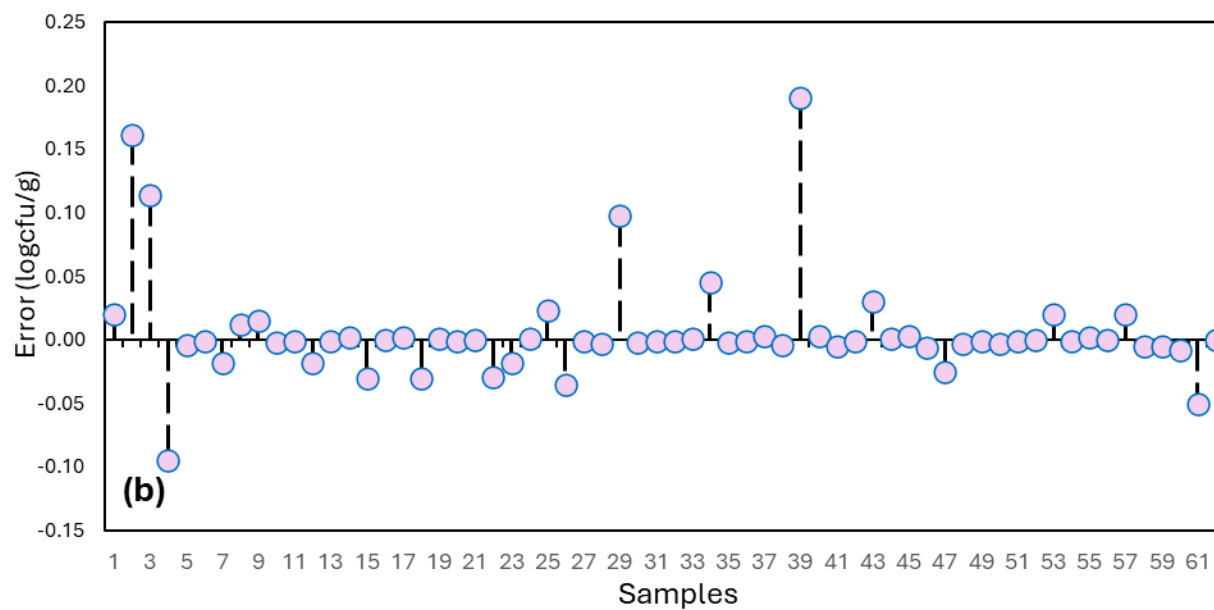
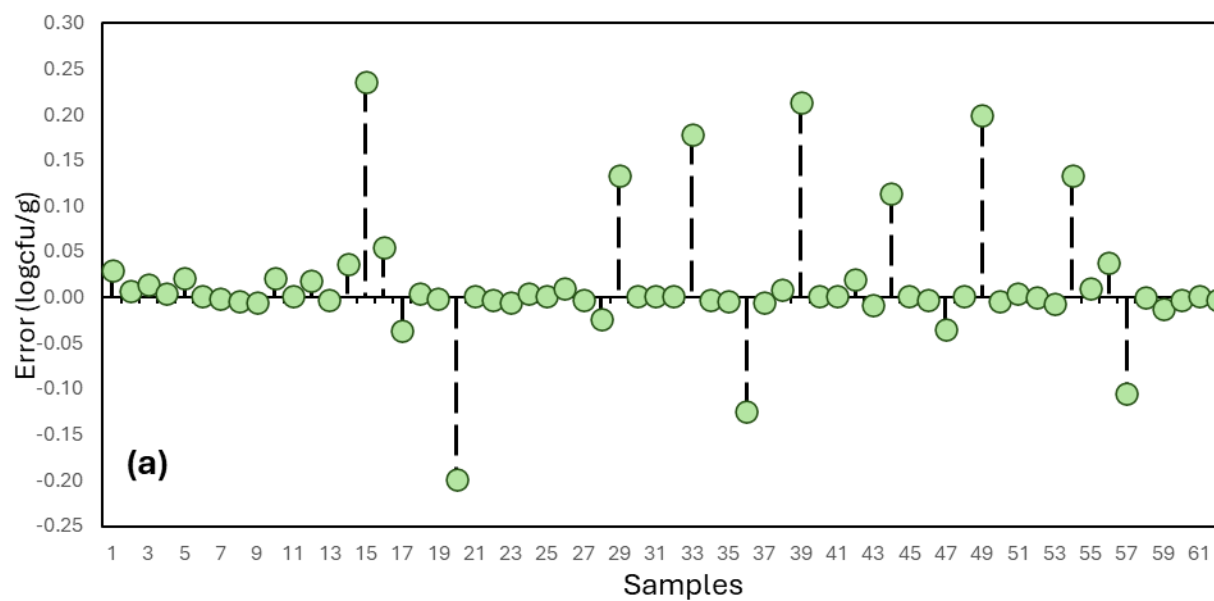


Figure 8. Correlation chart of ANN modeling results via experimental results in different conditions Based on the curve fitting of the results in Figure 8, a linear relationship between the outcomes has been identified, indicated by the good fit and the high correlation coefficient value, which is close to one. This suggests a direct relationship between the data.

Figure 9 illustrates the deviation of the predicted values from the actual values in the model, disaggregated by different measurement samples. Upon examining each of the measured samples, the prediction results for the microbial load reduction show an average error of 0.003 and a maximum error of 0.236.



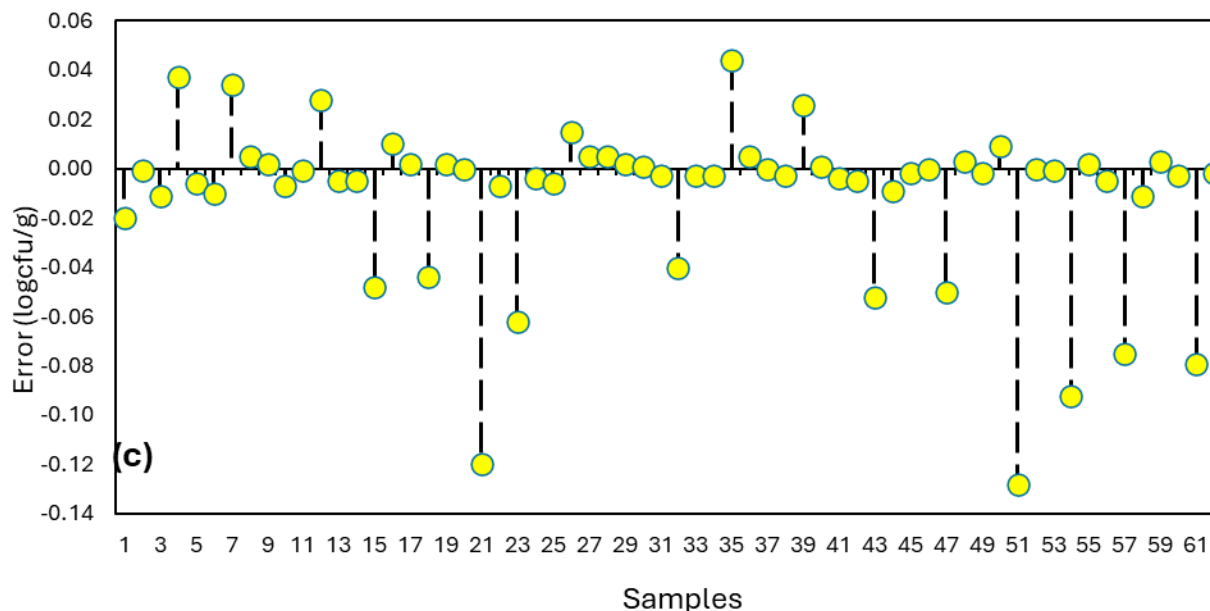


Figure 8. Deviation of the ANN-3 results for microbial load reduction relative to the actual values

a) Escherichia Coli Count (ECC) b) Bacillus Cereus Count (BCC) c) Mold Count (MC)

Conclusion

Plasma can be preferred over other methods for surface decontamination spices without causing significant quality damage. Non-thermal plasma is an effective source of active species and factors such as positive and negative ions, excited atoms, and molecules, which have the ability to inactivate and kill bacteria, viruses, and microorganisms without significant thermal effects. Dielectric Barrier Discharge (DBD) is a suitable source for generating non-thermal plasma at atmospheric pressure. In this study, the effect of plasma based on dielectric barrier discharge at atmospheric pressure with gases (air and nitrogen) on the microbiological, physicochemical, and sensory properties of the examined sumac samples was investigated, and the following results were obtained. Cold plasma was able to reduce microorganisms. The effect of cold plasma irradiation on microbial reduction was not uniform, with Gram-negative bacteria, such as Escherichia coli, showing the highest sensitivity, and molds showing the lowest sensitivity to

plasma irradiation. Using air as the input gas was more effective than nitrogen in reducing microbial load, and the duration of exposure led to a significant reduction in microbial load. However, the increase in duration had a negative effect on the active compounds of sumac, resulting in their reduction, with the maximum reduction in antioxidant activity observed at 15 minutes. According to the result of the ANN model, absolute mean error of 0.008% (much less than 10%), an RMSE of 0.029, a correlation coefficient of 99.8%, and a mean error of only +0.0002, this method suggested for prediction of microbial load and other parameters in food industrials. Based on the results obtained, it is recommended that researchers in future studies optimize the model using metaheuristic algorithms such as genetic algorithms, honey bee algorithms, etc., and compare their results with existing models.

References

- [1] J.X. Wong, S. Ramli, R. Son, A review: characteristics and prevalence of psychrotolerant food spoilage bacteria in chill-stored meat, milk and fish, *Food Res* 7 (2023) 23–32. [https://doi.org/10.26656/FR.2017.7\(1\).694](https://doi.org/10.26656/FR.2017.7(1).694).
- [2] D. Mandal, T. Sarkar, R. Chakraborty, Critical Review on Nutritional, Bioactive, and Medicinal Potential of Spices and Herbs and Their Application in Food Fortification and Nanotechnology, *Appl Biochem Biotechnol* 195 (2023) 1319–1513. <https://doi.org/10.1007/S12010-022-04132-Y>.
- [3] S. Nida, J.A. Moses, C. Anandharamakrishnan, Isochoric Freezing and Its Emerging Applications in Food Preservation, *Food Engineering Reviews* 13 (2021) 812–821. <https://doi.org/10.1007/S12393-021-09284-X>.
- [4] J. V. García-Pérez, J.A. Carcel, A. Mulet, E. Riera, R.R. Andrés, J.A. Gallego-Juárez, Ultrasonic drying for food preservation, *Power Ultrasonics: Applications of High-Intensity Ultrasound, Second Edition* (2023) 743–771. <https://doi.org/10.1016/B978-0-12-820254-8.00027-0>.
- [5] A. Veremachi, B.C. Cuamba, O.J. Nydal, J. Lovseth, A. Zia, Direct illuminated rock-bed heat storage a potential component of a solar thermal system for food preservation and space heating in rural areas of Mozambique, *ISES Solar World Congress 2015, Conference Proceedings* (2015) 1518–1526. <https://doi.org/10.18086/SWC.2015.02.13>.
- [6] N. Segueni, N. Boutaghane, S.T. Asma, N. Tas, U. Acaroz, D. Arslan-Acaroz, S.R.A. Shah, H.A. Abdellatieff, S. Akkal, R. Peñalver, G. Nieto, Review on Propolis Applications in Food Preservation and Active Packaging, *Plants* 12 (2023). <https://doi.org/10.3390/PLANTS12081654>.
- [7] C. Barry-Ryan, Physical and chemical methods for food preservation using natural antimicrobials, *Handbook of Natural Antimicrobials for Food Safety and Quality* (2015) 211–228. <https://doi.org/10.1016/B978-1-78242-034-7.00010-4>.

- [8] A. Sridhar, M. Ponnuchamy, P.S. Kumar, A. Kapoor, Food preservation techniques and nanotechnology for increased shelf life of fruits, vegetables, beverages and spices: a review, *Environ Chem Lett* 19 (2021) 1715–1735. <https://doi.org/10.1007/S10311-020-01126-2>.
- [9] H. Bagheri, S. Abbaszadeh, Effect of Cold Plasma on Quality Retention of Fresh-Cut Produce, *J Food Qual* 2020 (2020). <https://doi.org/10.1155/2020/8866369>.
- [10] J. de A. Bezerra, C.V. Lamarão, E.A. Sanches, S. Rodrigues, F.A.N. Fernandes, G.L.P.A. Ramos, E.A. Esmerino, A.G. Cruz, P.H. Campelo, Cold plasma as a pre-treatment for processing improvement in food: A review, *Food Research International* 167 (2023). <https://doi.org/10.1016/J.FOODRES.2023.112663>.
- [11] J.E. Kim, I.H. Kim, S.C. Min, Microbial decontamination of vegetables and spices using cold plasma treatments, *Korean Journal of Food Science and Technology* 45 (2013) 735–741. <https://doi.org/10.9721/KJFST.2013.45.6.735>.
- [12] S. Saremnezhad, M. Soltani, A. Faraji, A.A. Hayaloglu, Chemical changes of food constituents during cold plasma processing: A review, *Food Research International* 147 (2021) 110552. <https://doi.org/10.1016/J.FOODRES.2021.110552>.
- [13] M. Khoshkham, M.H. Shahrajabian, R.B. Singh, W. Sun, A. Magadlela, M. Khatibi, Q. Cheng, Sumac: a functional food and herbal remedy in traditional herbal medicine in the Asia, *Functional Foods and Nutraceuticals in Metabolic and Non-Communicable Diseases* (2021) 261–266. <https://doi.org/10.1016/B978-0-12-819815-5.00018-5>.
- [14] M.M. Ahmadian-Attari, G. Amin, M.R. Fazeli, H. Jamalifar, A review on antimicrobial activities of sumac fruit (*Rhus coriaria* L.), *Journal of Medicinal Plants* 7 (2008).
- [15] M. Akbari-Fakhrabadi, J. Heshmati, M. Sepidarkish, F. Shidfar, Effect of sumac (*Rhus Coriaria*) on blood lipids: A systematic review and meta-analysis, *Complement Ther Med* 40 (2018) 8–12. <https://doi.org/10.1016/J.CTIM.2018.07.001>.
- [16] G. Gollu, G.P. Gunaydin, A. Cakmak, A.M. Cakmak, Traditional nanny circumcision and dressing with sumac, onion and oil: A case report and review of the literature, *Journal of*

- Experimental and Clinical Medicine (Turkey) 36 (2019) 87–90.
<https://doi.org/10.5835/JECM.OMU.36.03.004>.
- [17] A. Ghafouri, M.D. Estêvão, P. Alibakhshi, A.B. Pizarro, A.F. Kashani, E. Persad, H. Heydari, M. Hasani, J. Heshmati, M. Morvaridzadeh, Sumac fruit supplementation improve glycemic parameters in patients with metabolic syndrome and related disorders: A systematic review and meta-analysis, *Phytomedicine* 90 (2021).
<https://doi.org/10.1016/J.PHYMED.2021.153661>.
- [18] İ. Kılınçer, L. Khanyile, K. Gürcan, Population structure of sumac (*Rhus coriaria* L.) from Türkiye based on transcriptome-developed SSR marker, *Genet Resour Crop Evol* 70 (2023) 1197–1213. <https://doi.org/10.1007/S10722-022-01497-1>.
- [19] M.M. Hassan, K. Saifullah, Sustainable dyeing and functionalization of jute fabric with a Chinese sumac gall-derived gallotannin using eco-friendly mordanting agents, *Cellulose* 28 (2021) 5055–5070. <https://doi.org/10.1007/S10570-021-03805-X>.
- [20] M. Mohit, M. Nouri, M. Samadi, Y. Nouri, N. Heidarzadeh-Esfahani, K. Venkatakrishnan, C. Jalili, The effect of sumac (*Rhus coriaria* L.) supplementation on glycemic indices: A systematic review and meta-analysis of controlled clinical trials, *Complement Ther Med* 61 (2021). <https://doi.org/10.1016/J.CTIM.2021.102766>.
- [21] K. Sakhr, S. El Khatib, Physicochemical properties and medicinal, nutritional and industrial applications of Lebanese Sumac (Syrian Sumac - *Rhus coriaria*): A review, *Heliyon* 6 (2020). <https://doi.org/10.1016/J.HELIYON.2020.E03207>.
- [22] S. Kumar, S. Pipliya, P.P. Srivastav, Effect of cold plasma processing on physicochemical and nutritional quality attributes of kiwifruit juice, *J Food Sci* 88 (2023) 1533–1552.
<https://doi.org/10.1111/1750-3841.16494>.
- [23] Y. Zhou, J. Li, Z. Li, Q. Ma, L. Wang, Extraction of anthocyanins from haskap using cold plasma-assisted enzyme, *J Sci Food Agric* 103 (2023) 2186–2195.
<https://doi.org/10.1002/JSFA.12349>.

- [24] S. Jaddu, S. Abdullah, M. Dwivedi, R.C. Pradhan, Multipin cold plasma electric discharge on hydration properties of kodo millet flour: Modelling and optimization using response surface methodology and artificial neural network – Genetic algorithm, *Food Chemistry: Molecular Sciences* 5 (2022). <https://doi.org/10.1016/J.FOCHMS.2022.100132>.
- [25] B. Paknezhad, M. Vakili, M. Bozorgi, M. Hajjalibabaie, M. Yahyaei, A hybrid genetic–BP algorithm approach for thermal conductivity modeling of nanofluid containing silver nanoparticles coated with PVP, *J Therm Anal Calorim* (2020). <https://doi.org/10.1007/s10973-020-09989-x>.
- [26] M. Yahyaei, M. Vakili, B. Paknezhad, Artificial brain structure-based modeling to predict the photo-thermal conversion performance of graphene nanoplatelets nanofluid using experimental data, *J Therm Anal Calorim* (2020). <https://doi.org/10.1007/s10973-020-10198-9>.
- [27] S. Riahi, E. Abedini, M. Vakili, M. Riahi, Providing an accurate global model for monthly solar radiation forecasting using artificial intelligence based on air quality index and meteorological data of different cities worldwide, *Environmental Science and Pollution Research* (2021) 1–28. <https://doi.org/10.1007/s11356-021-14126-8>.
- [28] L.A. Espinosa Sandoval, A.M. Polanía Rivera, L. Castañeda Florez, A. García Figueroa, Application of artificial neural networks (ANN) for predicting the effect of processing on the digestibility of foods, *Food Structure Engineering and Design for Improved Nutrition, Health and Well-Being* (2022) 333–361. <https://doi.org/10.1016/B978-0-323-85513-6.00011-6>.
- [29] D. Wang, M. Zhang, C.L. Law, L. Zhang, Natural deep eutectic solvents for the extraction of lentinan from shiitake mushroom: COSMO-RS screening and ANN-GA optimizing conditions, *Food Chem* 430 (2024). <https://doi.org/10.1016/J.FOODCHEM.2023.136990>.
- [30] K. Chen, M. Zhang, D. Wang, A.S. Mujumdar, D. Deng, Development of quinoa (*Chenopodium quinoa* Willd) protein isolate-gum Arabic conjugates via ultrasound-assisted wet heating for spice essential oils emulsification: Effects on water solubility, bioactivity,

- and sensory stimulation, *Food Chem* 431 (2024).
<https://doi.org/10.1016/J.FOODCHEM.2023.137001>.
- [31] Y. Ma, Y. Leng, D. Huo, D. Zhao, J. Zheng, P. Zhao, H. Yang, F. Li, C. Hou, A portable sensor for glucose detection in Huangshui based on blossom-shaped bimetallic organic framework loaded with silver nanoparticles combined with machine learning, *Food Chem* 429 (2023). <https://doi.org/10.1016/J.FOODCHEM.2023.136850>.
- [32] Z. Lu, J. Qin, C. Wu, J. Yin, M. Sun, G. Su, X. Wang, Y. Wang, J. Ye, T. Liu, H. Rao, L. Feng, Dual-channel MIRECL portable devices with impedance effect coupled smartphone and machine learning system for tyramine identification and quantification, *Food Chem* 429 (2023). <https://doi.org/10.1016/J.FOODCHEM.2023.136920>.
- [33] Y. Cui, W. Lu, J. Xue, L. Ge, X. Yin, S. Jian, H. Li, B. Zhu, Z. Dai, Q. Shen, Machine learning-guided REIMS pattern recognition of non-dairy cream, milk fat cream and whipping cream for fraudulence identification, *Food Chem* 429 (2023).
<https://doi.org/10.1016/J.FOODCHEM.2023.136986>.
- [34] L. Wang, X. Li, H. Zhu, Y. Zhao, Influencing factors of livestream selling of fresh food based on a push-pull model: A two-stage approach combining structural equation modeling (SEM) and artificial neural network (ANN), *Expert Syst Appl* 212 (2023).
<https://doi.org/10.1016/J.ESWA.2022.118799>.
- [35] Research on the design of green and low-carbon food packaging based on artificial intelligence technology, *Global NEST Journal* (2023).
<https://doi.org/10.30955/GNJ.004705>.
- [36] ISO 948:1980 - Spices and condiments — Sampling, (n.d.).
<https://www.iso.org/standard/5369.html> (accessed July 18, 2023).
- [37] ISO 6887-1:2017 - Microbiology of the food chain — Preparation of test samples, initial suspension and decimal dilutions for microbiological examination — Part 1: General rules for the preparation of the initial suspension and decimal dilutions, (n.d.).
<https://www.iso.org/standard/63335.html> (accessed July 18, 2023).

- [38] ISO 7251:2005 - Microbiology of food and animal feeding stuffs — Horizontal method for the detection and enumeration of presumptive *Escherichia coli* — Most probable number technique, (n.d.). <https://www.iso.org/standard/34568.html> (accessed July 18, 2023).
- [39] ISO 7932:2004/Amd 1:2020 - Microbiology of food and animal feeding stuffs — Horizontal method for the enumeration of presumptive *Bacillus cereus* — Colony-count technique at 30 degrees C — Amendment 1: Inclusion of optional tests, (n.d.). <https://www.iso.org/standard/76664.html> (accessed July 18, 2023).
- [40] ISO 21527-2:2008 - Microbiology of food and animal feeding stuffs — Horizontal method for the enumeration of yeasts and moulds — Part 2: Colony count technique in products with water activity less than or equal to 0,95, (n.d.). <https://www.iso.org/standard/38276.html> (accessed July 18, 2023).
- [41] G.S. Mittal, Artificial neural network based process modeling, Handbook of Farm, Dairy and Food Machinery Engineering (2019) 525–531. <https://doi.org/10.1016/B978-0-12-814803-7.00021-X>.
- [42] F. (Francesco) Ventriglia, Neural modeling and neural networks, Pergamon Press, 1994. <http://www.sciencedirect.com:5070/book/9780080422770/neural-modeling-and-neural-networks> (accessed July 8, 2023).
- [43] Artificial Neural Networks, (1992). <https://doi.org/10.1016/C2009-0-09010-2>.
- [44] Neural Networks Modeling and Control, Neural Networks Modeling and Control (2020). <https://doi.org/10.1016/C2018-0-01454-1>.
- [45] S. Mirjalili, Evolutionary Algorithms and Neural Networks, 780 (2019). <https://doi.org/10.1007/978-3-319-93025-1>.
- [46] M. Vakili, M. Yahyaei, J. Ramsay, P. Aghajannezhad, B. Paknezhad, Adaptive neuro-fuzzy inference system modeling to predict the performance of graphene nanoplatelets nanofluid-based direct absorption solar collector based on experimental study, Renew Energy 163 (2021) 807–824. <https://doi.org/10.1016/j.renene.2020.08.134>.

HOW TO CITE THIS ARTICLE

Somayeh Sepahvand, Nastaran Khalaj Zeighami, Samaneh Tayebi-Moghaddam, “**Experimental Investigation and Modelling of Cold Plasma Effect on Microbial Load Reduction of Sumac (*Rhus coriaria* L) by Artificial Neural Network with Levenberg–Marquardt Algorithm**” International Journal of New Chemistry., 2025; 12(4), 792-824.